

General Disclaimer

One or more of the Following Statements may affect this Document

- This document has been reproduced from the best copy furnished by the organizational source. It is being released in the interest of making available as much information as possible.
- This document may contain data, which exceeds the sheet parameters. It was furnished in this condition by the organizational source and is the best copy available.
- This document may contain tone-on-tone or color graphs, charts and/or pictures, which have been reproduced in black and white.
- This document is paginated as submitted by the original source.
- Portions of this document are not fully legible due to the historical nature of some of the material. However, it is the best reproduction available from the original submission.

(NASA-CR-169848) THE DETAILED CHEMISTRY AND
THERMODYNAMICS OF SODIUM IN OXYGEN-RICH
FLAMES (California Univ.) 27 p
HC A03/NP A01

N83-17626

63/25 Unclas
02727

WSCI 82-45

**THE DETAILED CHEMISTRY AND THERMODYNAMICS
OF SODIUM IN OXYGEN-RICH FLAMES**

A.J. Hynes,[†] M. Steinberg and K. Schofield
Quantum Institute, University of California
Santa Barbara, CA 93106



Presented at the Fall Meeting of the Western States Section
of the Combustion Institute held at
Sandia National Laboratories, Livermore
October 11 - 12, 1982

[†]Department of Physics, Oberlin College
Oberlin, Ohio 44074

ABSTRACT

Measurement of sodium and OH concentrations in ten oxygen-rich $H_2/O_2/N_2$ flames by respective saturated and low-power laser induced fluorescence techniques have permitted a detailed examination of the pronounced flame chemistry of sodium in such oxygen rich media. Previous interpretations have been shown to be largely incomplete or in error.

The flame downstream profiles indicate that the amount of free sodium tracks the decay of H-atom and as the flame radicals decay sodium becomes increasingly bound in a molecular form. A detailed kinetic model indicates that the sodium is distributed between NaOH and NaO_2 species. Concentrations of NaO are very small and NaH negligible. The actual distribution is controlled by the state of equilibration of the flames' basic free radicals. Na, NaO_2 and NaOH are all coupled to one another by fast reactions which can rapidly interconvert one to another as flame conditions vary. Above about 2000K, NaOH becomes dominant whereas NaO_2 plays an increasingly important contribution at lower temperatures.

The dissociation energy $D_0^0(Na-O_2)$ is established to be 35 ± 5 kcal mol^{-1} and the rate constant for the $Na+O_2+M$ reaction of $1 \times 10^{-31} cm^6 molecule^{-2} s^{-1}$, not incompatible with a recent flash photolysis measurement at lower temperatures. The rate constant for the reaction $NaOH+H = Na+H_2O$ approximates to its maximum allowed value based on gas kinetic hard-sphere collisions, $k = 1.1 \times 10^{-12} T^{1/2} cm^3 molecule^{-1} s^{-1}$.

INTRODUCTION

Although it is difficult to find a flame chemist who has not studied sodium, the flame chemistry of this ubiquitous atom has not been satisfactorily characterized under many common flame conditions. This is a consequence of our continuing inability to monitor directly molecular sodium species in flames. The subject of this presentation is the identification of the dominant chemistry accounting for the observed sodium disappearance profiles in a series of atmospheric pressure, lean (oxygen rich) $H_2/O_2/N_2$ flame gas flows of widely varying composition and temperature.

In rich $H_2/O_2/N_2$ flames sodium remains essentially in elemental form.^{1,2} Small amounts of NaOH formation can be expected via



which only becomes significant at temperatures above 2300K. In lean $H_2/O_2/N_2$ flames the decreased H-atom concentrations would favor slightly increased NaOH production.

Kaskan³ monitored Na and OH profiles in absorption in a series of lean, atmospheric pressure $H_2/O_2/N_2$ flames at 1400 to 1700K. He found reaction (12) not balanced and unable to account for the measured decays. Rather, he found the initial Na decay rates proportional to the O_2 concentration and suggested the three-body reaction



* Reaction numbering corresponds to ordering in the master list of reactions of Table II.

as the dominant Na oxidation process in these flames. His measured decay rates correspond to a value of about $10^{-33} \text{ cm}^6 \text{ molecule}^{-2} \text{ s}^{-1}$ for k_1 . McEwan and Phillips,⁴ in a subsequent study with temperatures ranging from 1380 to 2260K also monitored sodium in absorption but utilized the Li/LiOH method to measure H-atom. They found also that reaction (12) could not describe the observed Na decay profiles. However at temperatures above 2000K they concluded that reaction (1) was balanced and NaO_2 was the dominant sodium oxidation product. At lower temperatures it appeared to be too slow to become balanced. From the temperature dependence of a plot of $(\text{NaO}_2)/(\text{Na})(\text{O}_2)$ against T^{-1} they calculated a value of 65 kcal mol^{-1} for $D_0^0(\text{Na}-\text{O}_2)$. This value was found to have a computational error and later revised downward to $55.9 \text{ kcal mol}^{-1}$.⁵ From the initial Na decay rates in their flames McEwan and Phillips⁴ also determined values for k_1 of about $2 - 3 \times 10^{-33} \text{ cm}^6 \text{ molecule}^{-2} \text{ s}^{-1}$ in reasonable agreement with Kaskan's values.

In an extension of Kaskan's earlier effort, Carabetta and Kaskan⁶ examined the sodium oxidation in a series of lean flames as a function of pressure to evaluate the third body dependence of the Na disappearance rates. Over the temperature range from 1420 to 1500K at pressures from 100 to 1520 torr they found the initial rates of decay of sodium to be proportional to both O_2 and M concentrations supporting reaction (1) as the dominant sodium removal process.

Recently, Husain and Plane⁷ measured Na oxidation rates in a heated cell at 724 and 844K. They generated atomic Na by flash photolysis of NaI and followed the Na decay in absorption in the presence of He, N_2 , and CO_2 baths. They found the Na removal rate described by reaction (1) with a rate constant of about $10^{-30} \text{ cm}^6 \text{ molecule}^{-2} \text{ s}^{-1}$ with N_2 as the third body. This is 3 orders of magnitude faster than the reported measurements for k_1 in the previous flame studies. The unambiguity of the static cell measurements questions the assignment of the measured sodium decay rates in flames to reaction (1). Obviously some global overall process has been observed in flames that appears to behave as reaction (1).

Very recently, Jensen and Jones⁸ examined the catalysis of flame radical recombination rates by large quantities of sodium in a series of fuel-rich $H_2/O_2/N_2$ flames. They found they could explain the sodium catalyzed H-atom disappearance rates with reaction (12) along with



A computer fit to their measurements yielded a value of $5 \times 10^{-27} T^{-1} \text{ cm}^6 \text{ molecule}^{-2} \text{ s}^{-1}$ for k_{13} . This corresponds to $2.5 \times 10^{-30} \text{ cm}^6 \text{ molecule}^{-2} \text{ s}^{-1}$ at 2000K, unexpectedly large. Jensen⁹ then found that using reactions (12) and (13) he could account approximately for Kaskan's³ lean flame Na oxidation rates without recourse to the inclusion of NaO_2 . This, of course, eliminates the discrepancy existing between values for k_1 measured in flames and in the static cell. Jensen concluded that for reaction (1) to have a negligible contribution to the flame observations, but still be consistent with Husain and Plane's⁶ measurements, would require a value of about $40.6 \text{ kcal mol}^{-1}$ for $D_0^0(Na-O_2)$, about 15 kcal mol^{-1} below the revised value of Daugherty, McEwan and Phillips.⁵ However, this test by Jensen utilized the very limited data base provided by Kaskan which involves only two very similar flames. Our recent measurements on ten flames provides now the opportunity for a more extensive modeling of this system and a more critical test of Jensen's hypothesis.

EXPERIMENTAL

Most of the experimental system has been described previously^{10, 11} and will be very briefly discussed below. Flames were stabilized on a 2 cm dia. flat-flame Padley-Sugden burner¹² constructed of bundled hypodermic tubing. The burner is manifolded such that separate metered $H_2/O_2/N_2$ flows can be fed to an inner bundle, 1 cm dia., and to the outer bundle. An aerosol of aqueous sodium chloride was added to the central burner core by passage of a few $cm^3 sec^{-1}$ of N_2 through an ultrasonic nebulizer.¹³ Atomic sodium is rapidly generated in the flame reaction zone and is introduced at a rate to produce concentrations of about $10^{10} cm^{-3}$ in the hot flame gases.

The optical arrangement is illustrated in Fig. 1. A Nd-YAG (Quanta Ray DCR-PDL-1) pumped tunable dye laser was used to monitor Na and OH in fluorescence. A calibrated brightness temperature tungsten ribbon lamp was used for sodium line reversal measurements of flame temperatures.

The laser beam, about 1 mm dia., was passed through the flame and fluorescence sampled at right angles with an $f/5.3$ spherical mirror to match the monochromator aperture. The sampled beam was passed through a two mirror image rotator and into the entrance slit of an 0.35 m monochromator (McPherson 218). The detection optics image a section of the horizontal laser beam into the vertical monochromator slit with unity magnification. Thus, using a $50 \mu m$ slit that is 0.5 cm high, we detect an 0.5 cm length of beam fluorescence, near flame center, with a flame height resolution of the order of $100 \mu m$. The burner was mounted on a platform that was raised or lowered relative to the system optical axes to obtain time dependent profiles of properties above the flame front which is positioned close to the burner.

Sodium fluorescence measurements were made by saturating the sodium 589.0 nm ($^2S_{1/2} - ^2P_{3/2}$) transition and monitoring the closely coupled ($^2S_{1/2} - ^2P_{1/2}$) fluorescence. Under saturated conditions the fluorescence is insensitive to quenching and variations in laser power. With the short (6 ns) laser pulse there is insufficient time for either laser induced chemistry¹¹ or ionization of the sodium.¹⁴ In this manner the

ORIGINAL PAGE IS
OF POOR QUALITY

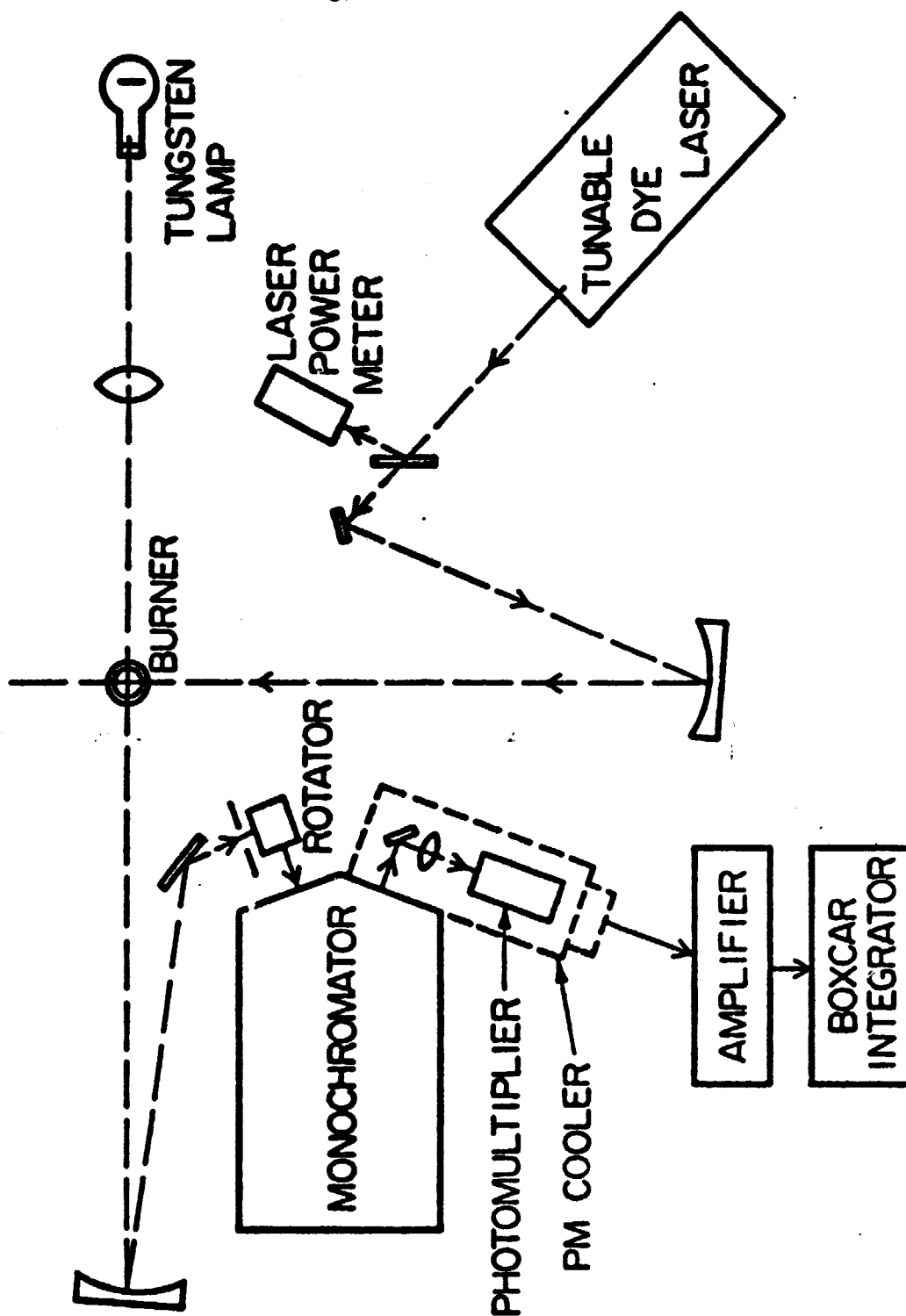
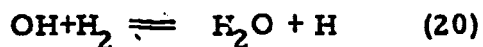
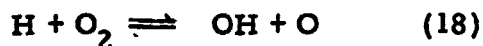


Figure 1. Experimental arrangement for laser induced fluorescence and line reversal temperature measurements.

relative fluorescence intensities were proportional to the atomic sodium concentrations. Relative concentration measurements were adequate for this study.

Absolute OH concentrations were measured in fluorescence using our previously established experimental conditions.^{10, 14, 15} The OH($A^2\Sigma^+ - X^2\Pi$) (1, 0), $R_1(6)$ transition at 281.14 nm was excited and fluorescence detected at 314.69 nm for the (1, 1) $Q_1(7)$ transition. The doubled output from the dye laser (using an R590 dye) was attenuated to produce fluorescence in the low power regime where fluorescence intensity is proportional to laser power. These relative intensity measurements were rendered quantitative by calibrating against OH fluorescence measurements in a high temperature fully equilibrated flame ($H_2/O_2/N_2 = 4/1/2$) for which the OH concentration is readily calculated.

The concentrations of the other flame radicals and trace flame constituents, (H), (O), and (H_2) were calculated assuming balanced chemistry in reactions (18), (19), and (20)



Kinetic calculations confirmed the ability of these processes to remain balanced throughout the flames employed in the study.

A flame matrix was employed to cover a wide range of compositions and temperatures. Flames studied are listed in Table I. These encompass a 750K temperature range from about 1650 to 2400K. In the hot flame gases the two major species H_2O and O_2 have concentrations that vary by factors of $\times 1.2$ and $\times 24$ fold, respectively, over this range of flames. In all cases significant departures from equilibrium are apparent for the flame radicals with extensive decay occurring over the first few milliseconds of the burnt gas region.

Table I. Experimental flame matrix and some major flame properties.

$H_2 / O_2 / N_2$		TEMPERATURE K	H_2O	O_2 Molecule cm^{-3}	OH
0.6	1 1	1906 - 1929	1.0 (18)	1.2 (18)	0.7 - 3.8 (16)
1	1 2	2066 - 2100	9.9 (17)	4.8 (17)	1.1 - 3.8 (16)
1	1 3	1667 - 1730	9.5 (17)	4.7 (17)	0.3 - 3.7 (16)
1.4	1 3	2152 - 2197	9.8 (17)	2.0 (17)	1.4 - 3.5 (16)
1.4	1 4	1828 - 1847	9.8 (17)	2.1 (17)	0.5 - 3.6 (16)
1.4	1 5	1654 - 1669	9.3 (17)	2.0 (17)	0.3 - 3.6 (16)
1.8	1 3	2320 - 2400	1.1 (18)	5.9 (16)	1.9 - 4.0 (16)
1.8	1 4	2145 - 2228	9.8 (17)	5.1 (16)	1.4 - 3.6 (16)
1.8	1 5	1862 - 1916	1.0 (18)	5.3 (16)	0.7 - 3.2 (16)
1.8	1 6	1703 - 1726	9.7 (17)	5.2 (16)	0.4 - 3.1 (16)
RANGE		750 K	x1.2	x24	x12

ORIGINAL PAGE IS
OF POOR QUALITY

MEASURED CONCENTRATION PROFILES

The concentrations of free sodium have been obtained as a function of distance (time) throughout the burnt gas regions of the ten oxygen rich flames. The fluorescence intensities have to be corrected solely for the differing flow volumes of each flame because the same rate of addition of sodium is made to each. Resulting concentrations over the first 4 ms region are indicated in Figure 2 for selected flames. These indicate the pronounced decays as observed previously.^{3,4} The decay shapes vary from flame to flame. This behavior is markedly different from that in fuel rich hydrogen or acetylene flames where the sodium remains almost totally in its free atomic state with only slight losses due to some NaOH formation and to diffusion. At these temperatures, for our purposes, thermal ionization is negligible on this time scale. Molecular formation is quite evident, becoming especially pronounced for certain flame compositions. Also, there is the suggestion that each flame starts in the reaction zone region from the same level of totally free atomic sodium which is then subject to its specific rate of depletion.

Corresponding OH concentrations in these flames are illustrated in Figure 3. Based on our earlier developed technique for quantitative low-power laser induced fluorescence measurements,^{10, 14, 15} which have been shown to be valid for fuel rich flames, this present series of measurements appear similarly valid.

Numerical kinetic calculations concerning the detailed balance among the minor flame species in oxygen rich flames, namely for OH, H, O and H₂, indicate, as under fuel-rich conditions, that there is sufficient time for these radicals to become interrelated in the burnt gas regions. By considering reactions (18), (19), and (20) it can be shown that, in the present time frame, changes in the concentration of one radical will immediately reflect through to the others. Consequently, from measured OH concentrations it is possible to calculate the corresponding amounts of H, O, and H₂ from the appropriate equilibrium constants and concentrations of H₂O and O₂. These latter two major species are largely unperturbed from their equilibrium concentration

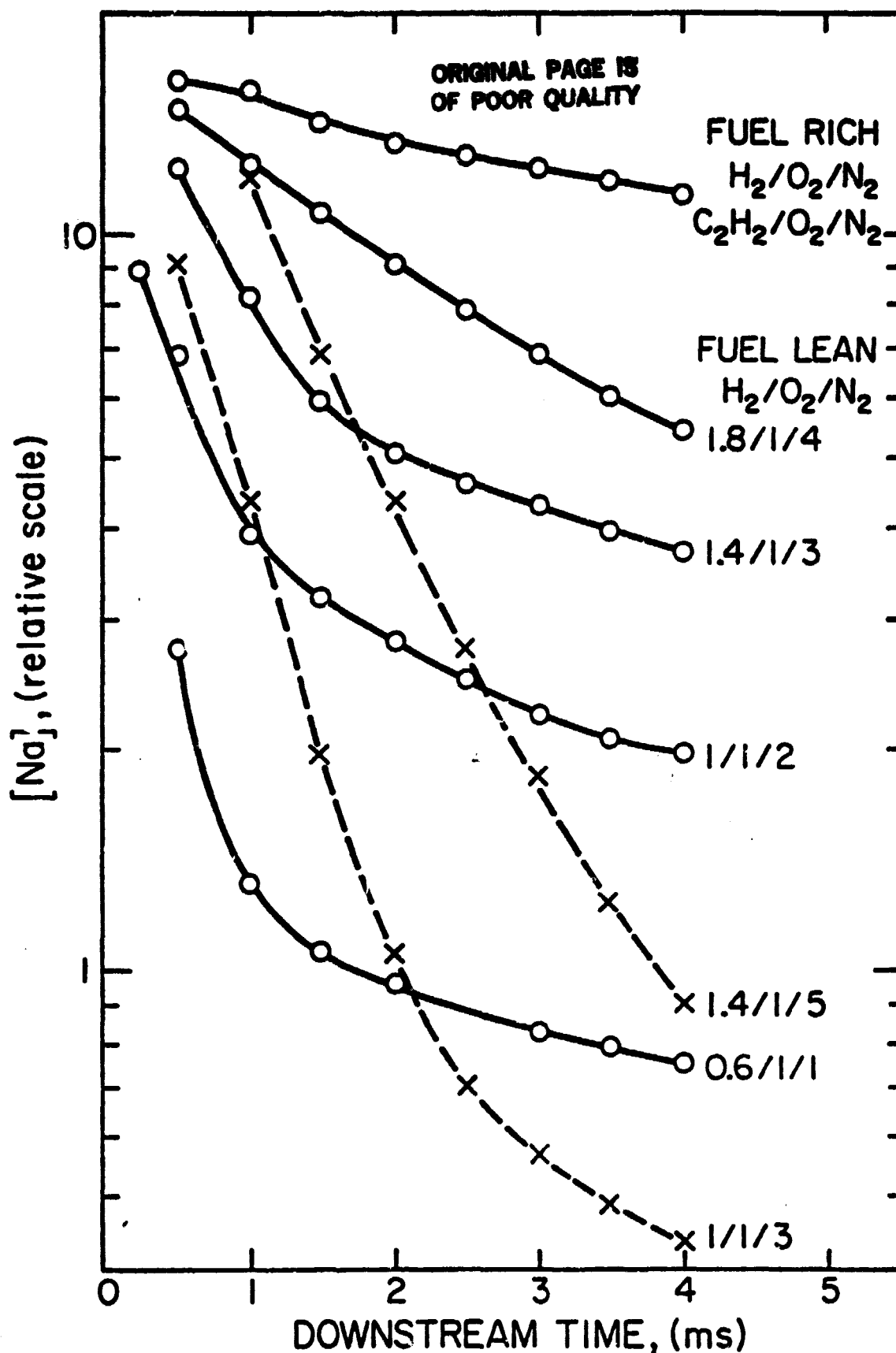


Figure 2. Measured atomic sodium concentrations in the burnt gases of several oxygen-rich hydrogen flames. Total sodium input approximates to 10^{10} atoms cm^{-3} .

ORIGINAL PAGE IS
OF POOR QUALITY

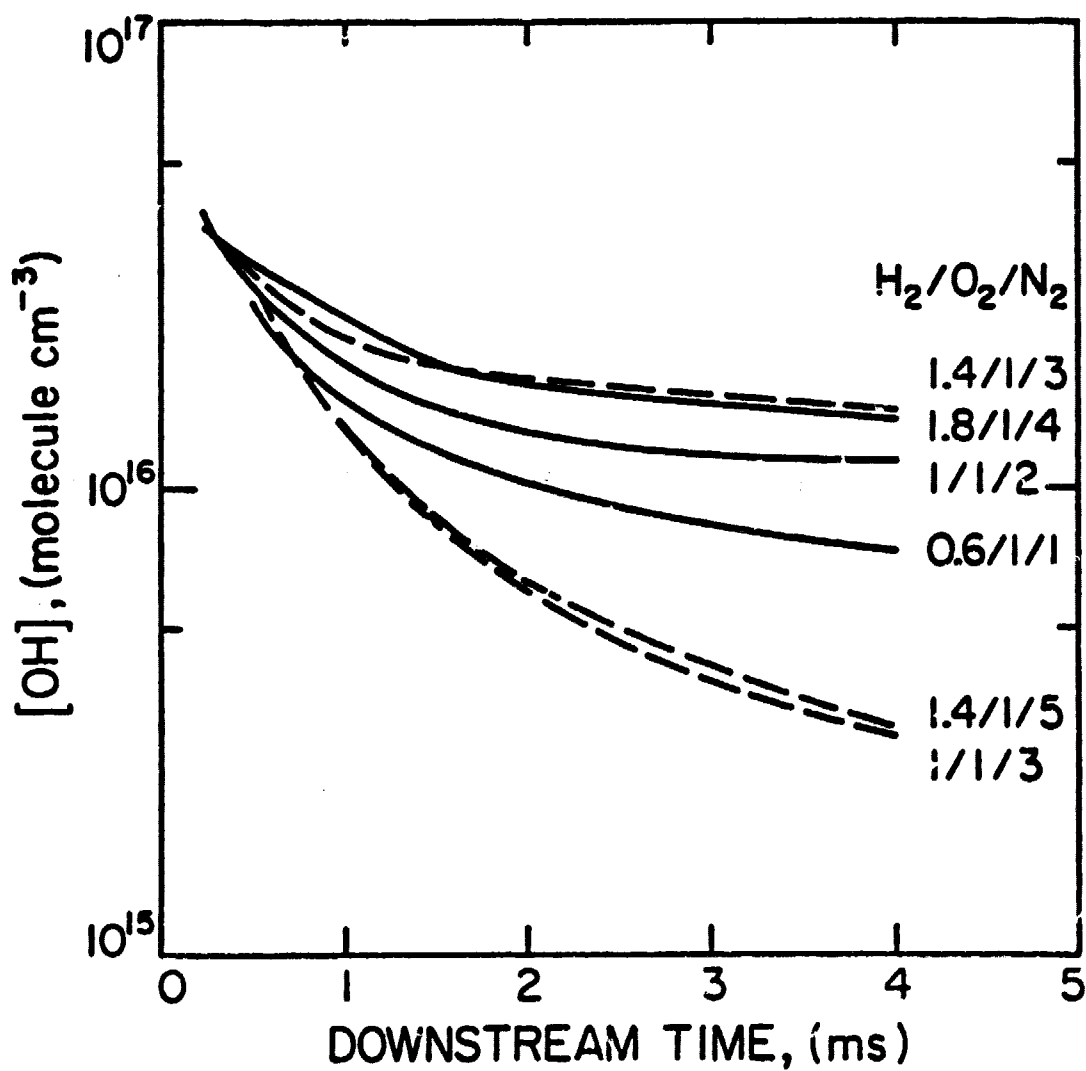


Figure 3. Experimentally measured OH concentrations in the burnt gases of several oxygen-rich hydrogen flames.

values and so can be calculated by an equilibrium code at the measured flame temperature. In this way, the following expressions can be derived:

$$[H] = \frac{K_{20} [OH]^3}{K_{18} K_{19} [O_2] [H_2O]}, \quad [O] = \frac{K_{20} [OH]^2}{K_{19} [H_2O]},$$

$$[H_2] = \frac{[OH]^2}{K_{18} K_{19} [O_2]}.$$

The relationship between OH and H is markedly different from fuel-rich behavior where $[OH] \propto [H] \propto [O]^{1/2} \propto [O_2]^{1/2}$. This is apparent in the shapes and magnitudes of the $[H]$ decays in Figure 4 calculated from the corresponding measured OH concentrations of Figure 3. Also, it may be noted that the more pronounced decay of $[H]$ is remarkably similar to that of the sodium decays of Figure 2. Clearly, there is some correlation between Na and H with the sodium decay obviously tracking that of the H-atom. This behavior, similarly observed in a previous study of the laser induced chemistry of sodium,¹¹ suggests the presence of a steady state distribution that readjusts as the radicals decay.

It does seem apparent therefore that the initial rates of decay of sodium are not a measure of the progress of the three body $Na + O_2 + M$ reaction as suggested by Kaskan³ and McEwan and Phillips⁴ and so cannot lead to a meaningful value for its rate constant. If anything, the sodium decay is more closely related to the H-atom decay, which is predominantly controlled by the three-body $H + O_2 + M \rightarrow HO_2 + M$ reaction in these flames. It seems probable that the observed dependence on O_2 and M concentrations of these initial sodium rates of decay⁶ was a consequence of this $H + O_2 + M$ reaction rather than an indication of the occurrence of the $Na + O_2 + M$ reaction. This further indicates the care required in interpreting such flame profiles and emphasizes the need to measure as many species in as wide a range of differing flame compositions and temperatures as is possible.

ORIGINAL PAGE IS
OF POOR QUALITY

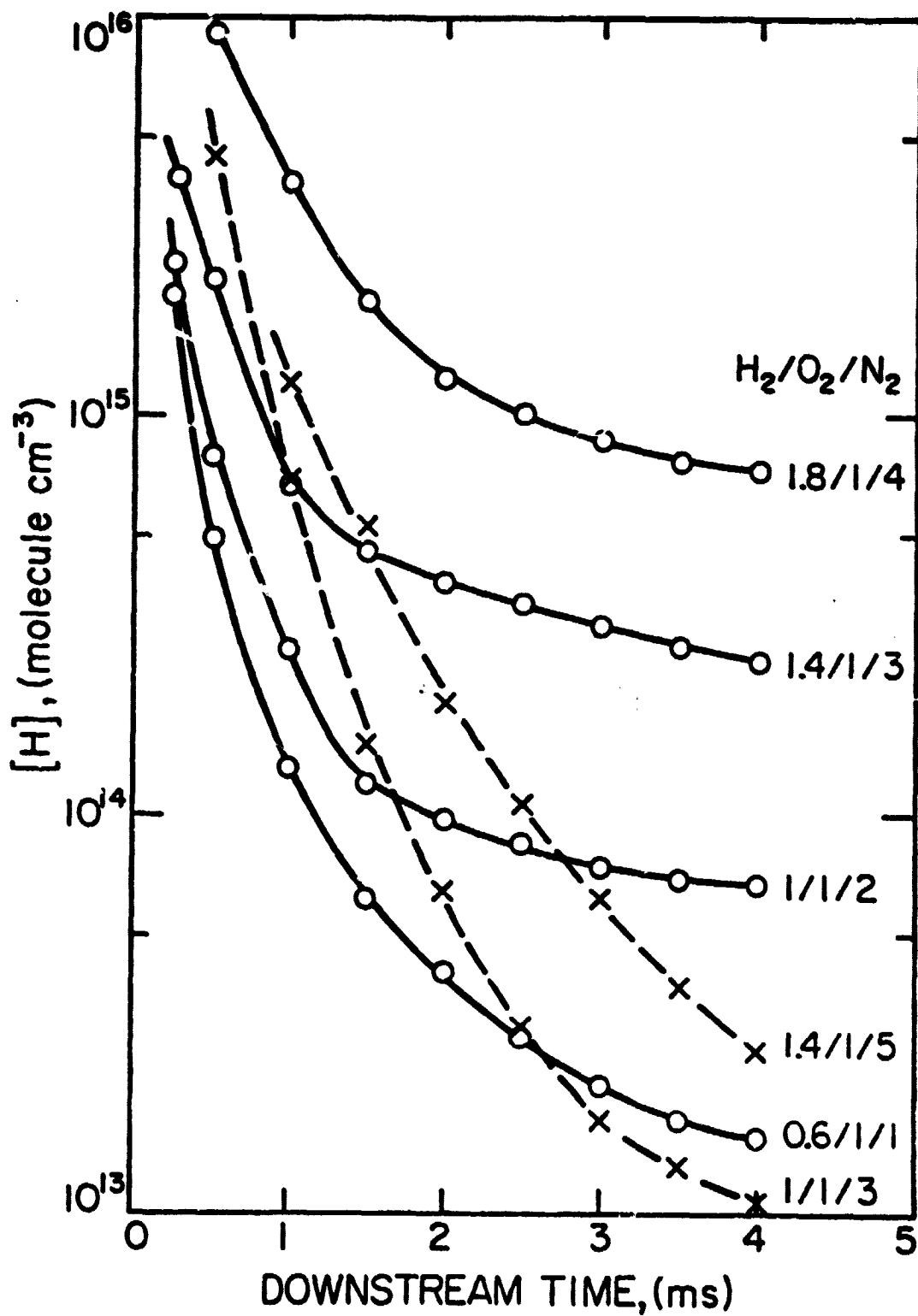


Figure 4. H-atom concentrations calculated from the measured OH concentrations.

KINETIC MODELING

McEwan and Phillips⁴ assumed the predominance of NaO_2 and its equilibration via reaction (1) in their brief study of this system. Using our more extensive data base we have tested this hypothesis by calculating the equilibrium constant of this reaction at points throughout each of the flames assuming that loss of sodium is due totally to NaO_2 formation. The result is indicated in Figure 5. The expected straight line corresponding to a $D_0^\circ(\text{Na-O}_2)$ $55.9 \text{ kcal mol}^{-1}$ is not confirmed. The departures in each flame clearly indicate that flame radicals are involved. A similar test of the dominance of NaOH via the balanced reaction (12) is illustrated in Figure 6 together with the expected equilibrium constant calculated from the JANAF tables. Behavior above and below 2000K appears to be significantly different. Above 2000K an approximate relationship does appear reasonable. However, below 2000K departures are such as to suggest the participation again of supplemental chemistry that involves the radical species whose concentrations significantly vary with time. The system is obviously more complex than previously considered and a more complete kinetic modeling is necessary.

A model has been analyzed involving all the possible reactions of Na , NaO , NaO_2 and NaOH in an H_2/O_2 flame environment. These are listed in Table II and schematically illustrated in Figure 7. An examination of the possible reactions of NaH indicate that it will be negligible in oxygen-rich flames and is not included. Also, due to the very low concentrations of sodium, molecules containing more than one atom of sodium cannot form. No reliable value exists for the $\Delta H_f(\text{NaO}_2)$ and the effect of this variable on the respective reaction enthalpies is included. At first sight, the possibility of handling such a large number of reactions seems questionable due to the fact that rate constants are available only for k_1 , k_{12} and k_{-12} .^{7, 11} However, a closer examination immediately leads to various significant conclusions and indicates that more than half of the reactions listed play a negligible role. Comparison to the analogous reactions where H replaces Na shows that it is not unreasonable to expect reactions (3), (4), (7), (9), (10), (16) and (17) to have preexponential rate constant factors that correspond to hard sphere gas kinetic collision frequencies. Consequently, in the initial

ORIGINAL PAGE IS
OF POOR QUALITY

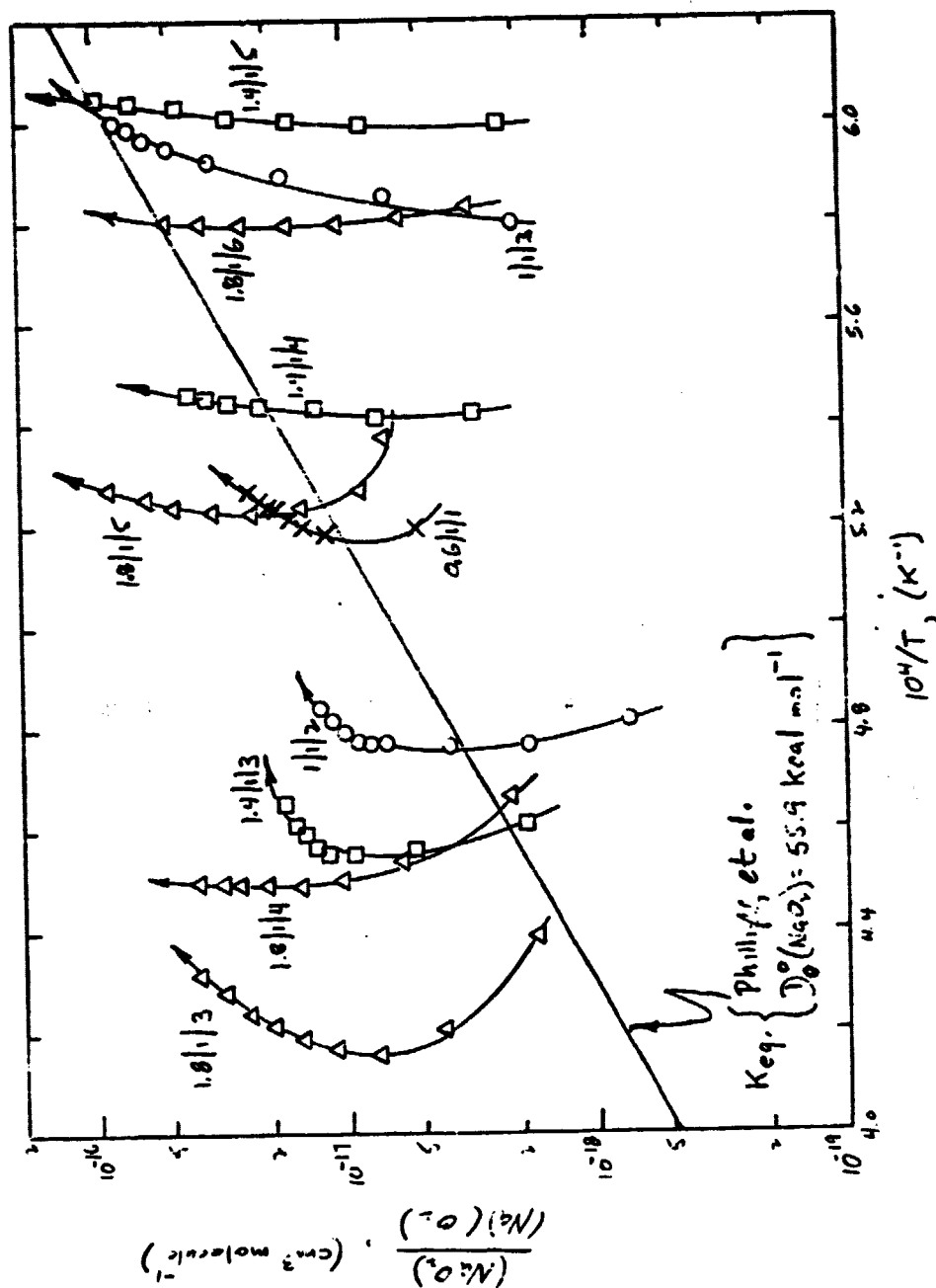


Figure 5. Equilibrium constant plot testing for the predominant molecular formation of NaO_2 via the $\text{Na} + \text{O}_2 + \text{M} \rightleftharpoons \text{NaO}_2 + \text{M}$ reaction. For each flame, marked by its $\text{H}_2/\text{O}_2/\text{N}_2$ ratio, individual points refer to downstream times of 0.25, 0.5, 1.0, 1.5, 2.0, 2.5, 3.0, 3.5, 4.0 ms, time increasing in the direction of the arrow.

ORIGINAL PAGE IS
OF POOR QUALITY

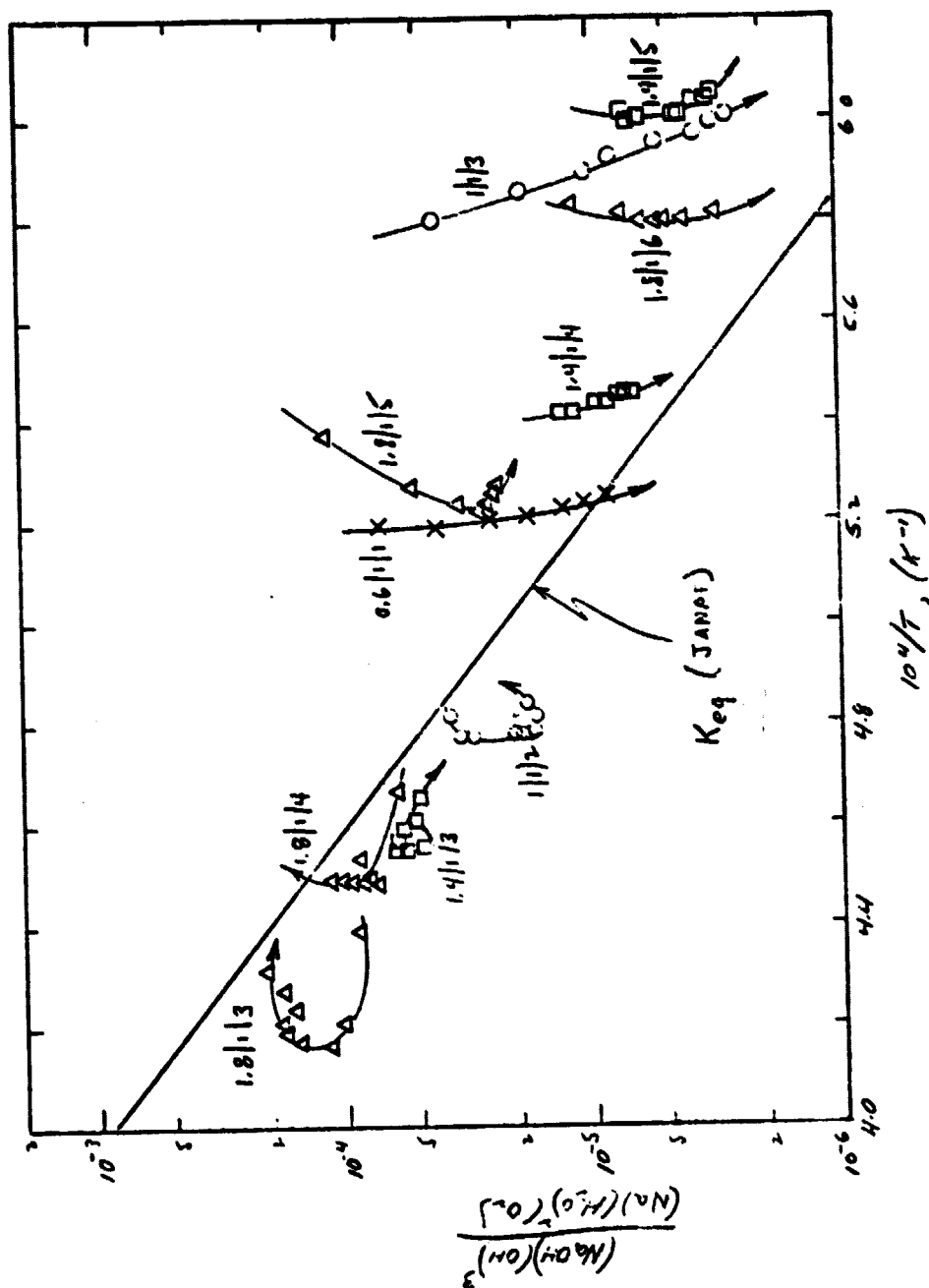


Figure 6. Equilibrium constant plot testing for the predominant molecular formation of NaOH via the $\text{Na} + \text{H}_2\text{O} \rightleftharpoons \text{NaOH} + \text{H}$ reaction. For each flame, marked by its $\text{H}_2/\text{O}_2/\text{N}_2$ ratios, individual points refer to downstream times of 0.25, 0.5, 1.0, 1.5, 2.0, 2.5, 3.0, 3.5, 4.0 ms, time increasing in the direction of the arrow.

Table II. List of potential reactions of Na, NaO,
NaO₂ and NaOH in H₂/O₂ flames.

	Reaction	$\Delta H^{\circ}(2000K) \text{ kcal mol}^{-1}$
1, -1	$\text{Na} + \text{O}_2 + \text{M} = \text{NaO}_2 + \text{M}$	$-(D_0^{\circ} + 1.16)$
2, -2	$\text{NaO}_2 + \text{H} = \text{Na} + \text{HO}_2$	$-(53.56 - D_0^{\circ})$
3, -3	$\text{NaO}_2 + \text{H} = \text{NaO} + \text{OH}$	$-(45.98 - D_0^{\circ})$
4, -4	$\text{NaO}_2 + \text{O} = \text{NaO} + \text{O}_2$	$-(61.54 - D_0^{\circ})$
5, -5	$\text{NaO}_2 + \text{OH} = \text{NaO} + \text{HO}_2$	$+(D_0^{\circ} - 9.78)$
6, -6	$\text{NaO}_2 + \text{H} = \text{NaOH} + \text{O}$	$-(64.51 - D_0^{\circ})$
7, -7	$\text{NaO}_2 + \text{OH} = \text{NaOH} + \text{O}_2$	$-(80.07 - D_0^{\circ})$
8, -8	$\text{NaOH} + \text{OH} = \text{NaO} + \text{H}_2\text{O}$	$+1.89$
9, -9	$\text{NaOH} + \text{H} = \text{NaO} + \text{H}_2$	$+16.55$
10, -10	$\text{NaOH} + \text{O} = \text{NaO} + \text{OH}$	$+18.53$
11, -11	$\text{NaOH} + \text{O}_2 = \text{NaO} + \text{HO}_2$	$+70.29$
12, -12	$\text{Na} + \text{H}_2\text{O} = \text{NaOH} + \text{H}$	$+41.90$
13, -13	$\text{Na} + \text{OH} + \text{M} = \text{NaOH} + \text{M}$	-81.23
14, -14	$\text{Na} + \text{HO}_2 = \text{NaOH} + \text{O}$	-10.95
15, -15	$\text{Na} + \text{OH} = \text{NaO} + \text{H}$	$+43.78$
16, -16	$\text{Na} + \text{HO}_2 = \text{NaO} + \text{OH}$	$+7.59$
17, -17	$\text{Na} + \text{O}_2 = \text{NaO} + \text{O}$	$+59.34$

D_0° represents $D_0^{\circ}(\text{Na}-\text{O}_2)$

Reaction number: + forward reaction, - reverse reaction.

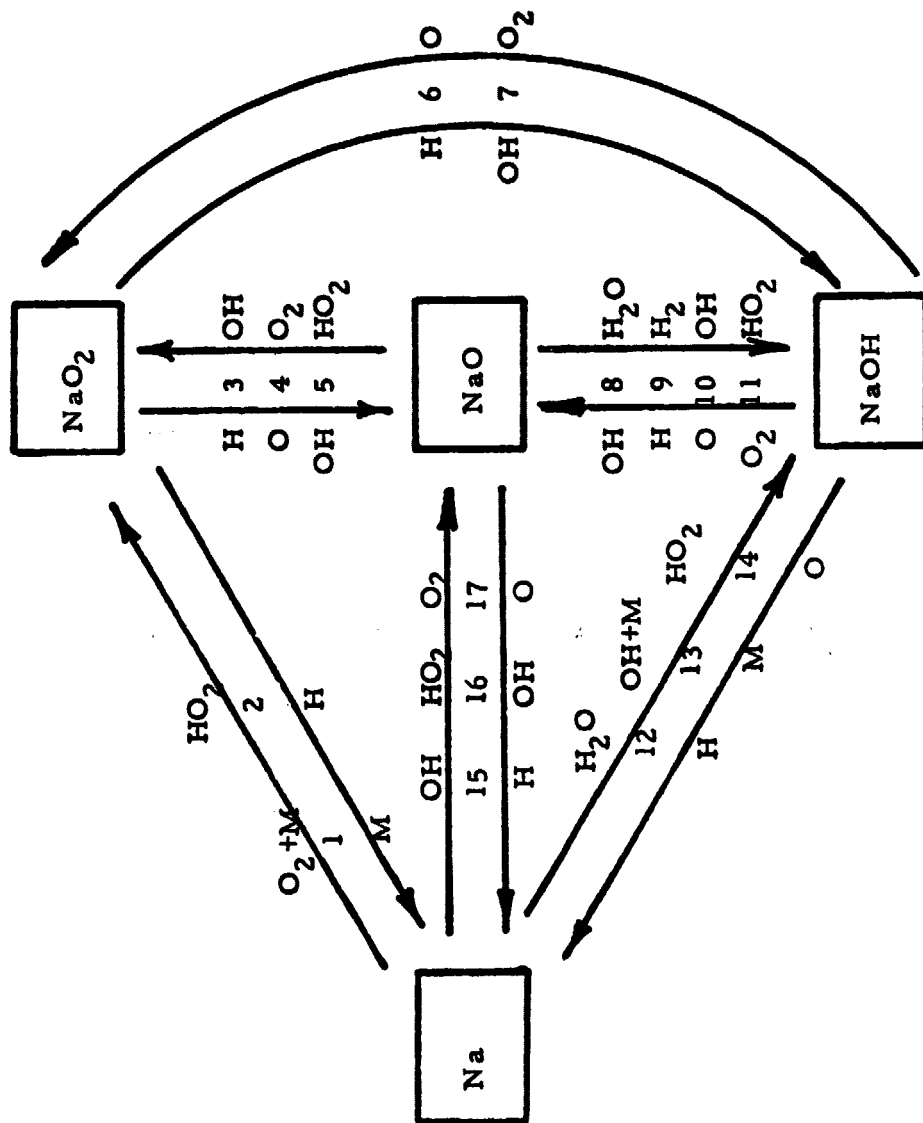


Figure 7. Reaction scheme including all the possible reactions listed in Table II that couple Na, NaO₂, NaO and NaOH. Specific reactants involved are indicated on the connecting arrows. Reaction number refers to Table II.

analysis all reaction rates have been set at their gas kinetic equivalent value suitably modified in the appropriate direction by the equilibrium constant. The required equilibrium constant for NaO_2 has been calculated based on a 105° bent structure with $r_e(\text{Na}-\text{O})$ 0.20 nm, $r_e(\text{O}-\text{O})$ 0.13 nm¹⁶ and vibrational frequencies of 1094, 391 and 333 cm^{-1} .^{17,18} Any uncertainties in this K_{NaO_2} value are in fact only of specific concern to reactions (3), (4), (6) and (7) and should not introduce significant errors.

An analysis of the time constants of these reactions confirms that the ms time frame provides a sufficient time for the establishment of a steady state distribution. Closer examination of the kinetic model immediately indicates the implications of Husain and Plane's⁷ value of $1.0 \times 10^{-30} \text{ cm}^6 \text{ molecule}^{-2} \text{ s}^{-1}$ for k_1 . Such a value predicts a severe depletion of Na that is too large to be compensated for unless $D_0^\circ(\text{Na}-\text{O}_2)$ is drastically reduced from its previously reported value of 55.9 kcal mol^{-1} . Also the flux coupling NaOH to NaO is so large that their distribution will be described very closely by the balance of reaction (8), suggesting that NaO will contribute at the most only a few percentage to the total molecular formation.

A test of the participation of only Na/ NaO_2 and Na/ NaOH reactions shows an unreasonable fit to the sodium curves of Figure 2, even when $D_0^\circ(\text{Na}-\text{O}_2)$ is drastically reduced and the appropriate rate constants are varied within reasonable bounds. Clearly some direct coupling between NaO_2 and NaOH is required to adjust calculated to experimental Na values.

Computer fitting of the model to the data has indicated that the most sensitive parameters are $D_0^\circ(\text{Na}-\text{O}_2)$ and k_1 . Unless the bond strength is reduced to 35 kcal mol^{-1} , and appears fixed to better than $\pm 5 \text{ kcal mol}^{-1}$, and k_1 is reduced to $10^{-31} \text{ cm}^6 \text{ molecule}^{-2} \text{ s}^{-1}$, it seems impossible to fit all flames to the data. Both shape and magnitude have to be reproduced which is quite demanding even though numerous parameters can be adjusted.

Our preliminary optimum fit for three of the flames is indicated in Figure 8. Refinements are still in progress and we expect to complete this program very soon.

ORIGINAL PAGE IS
OF POOR QUALITY

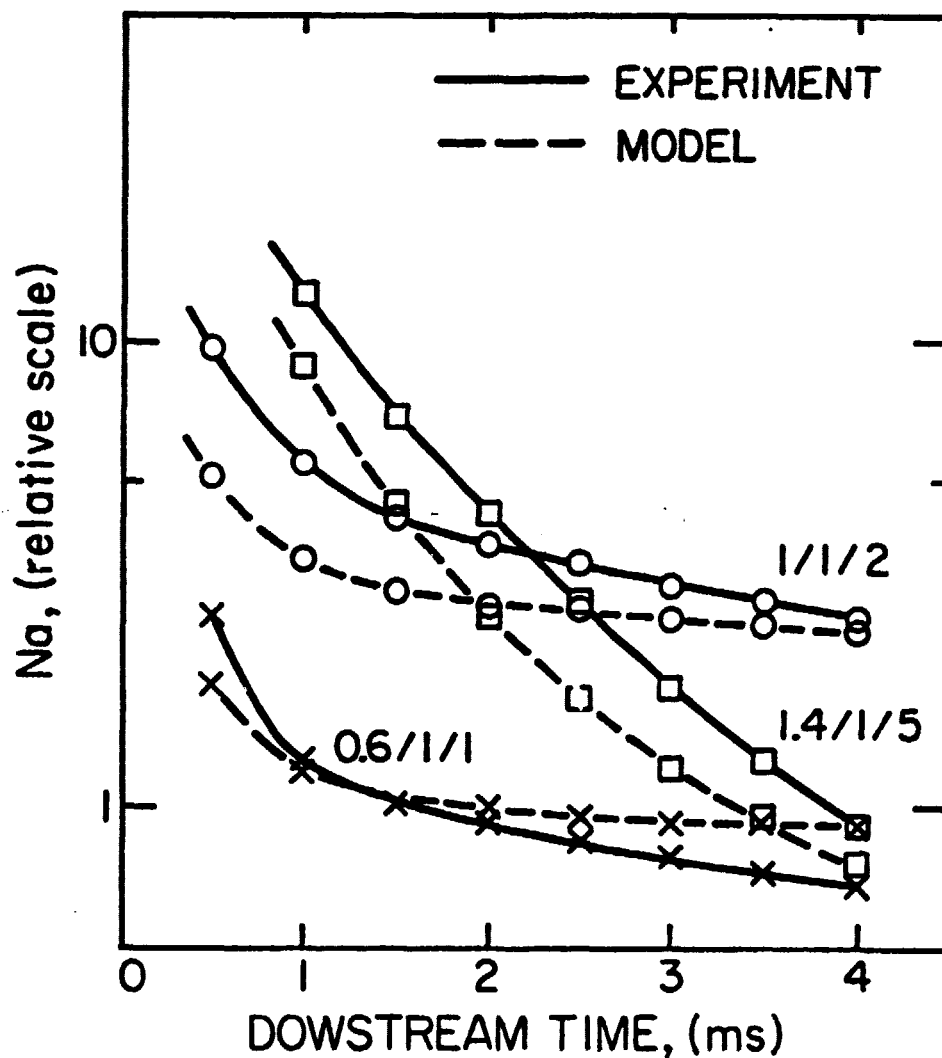
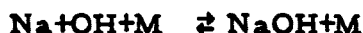


Figure 8. Optimized fit of the complete kinetic model to the experimental sodium concentrations, $D_0^0 = 35 \text{ kcal mol}^{-1}$, $k_1 = 10^{-31} \text{ cm}^6 \text{ molecule}^{-1} \text{ s}^{-1}$.

The calculations indicate that of the various reactions Na and NaO_2 are coupled predominantly via reaction (1) and reaction (2) is negligible. Direct coupling between Na and NaO is negligible and reactions (15)–(17) can be ignored. Na and NaOH are coupled by the well established reaction (12) which is known to be efficient. Due to the fast coupling between NaO and NaOH through reaction (8) the rates of (9)–(11) do not have any control in the model. In the other branches, reactions (3), (6) and (7) appear important and runs testing the sensitivity to their rate constants are in progress. It seems unlikely that the model will be able to distinguish between the indirect conversion of NaO_2 to NaOH via NaO or the direct channels.

It is clear that a simplified mechanism involving the seven reactions, (1), (3), (4), (6), (7), (8) and (12), fits the data quite well. Large values for the rate constants of most of these are found necessary.

Recently, the apparent discrepancy between Husain and Plane's measurement of k_1 and Kaskan's flame analysis has been realized by Jensen.⁹ Postulating that NaO_2 plays a negligible role, he has suggested in a reinterpretation of Kaskan's limited flame data that the reactions (12) and (13), namely



are sufficient to explain the main features of the flame data. A rather large rate constant of $5 \times 10^{-27} \text{ T}^{-1} \text{ cm}^6 \text{ molecule}^{-2} \text{ s}^{-1}$ is suggested for the three body formation of NaOH. This is two orders of magnitude faster than the corresponding H-analog reaction used in our analysis. Although open to possible uncertainty, it might be noted that k_1 also appears to be much faster than might have been expected.

Testing Jensen's hypothesis on our larger set of data confirms our own conclusion that a more complete chemistry must be considered. Utilizing the rate constants suggested by Jensen shows a poor fit to the data, in both shape and magnitude, as indicated for two flames in Figure 9. Modifications to the rate constants of the two reactions, although improving the fit, shows an inability to provide an acceptable agreement. The reason for the inadequacy of the model may be illustrated from plots of the molecular distributions predicted from our optimum fit to the more complete kinetic scheme. As seen

ORIGINAL PAGE IS
OF POOR QUALITY

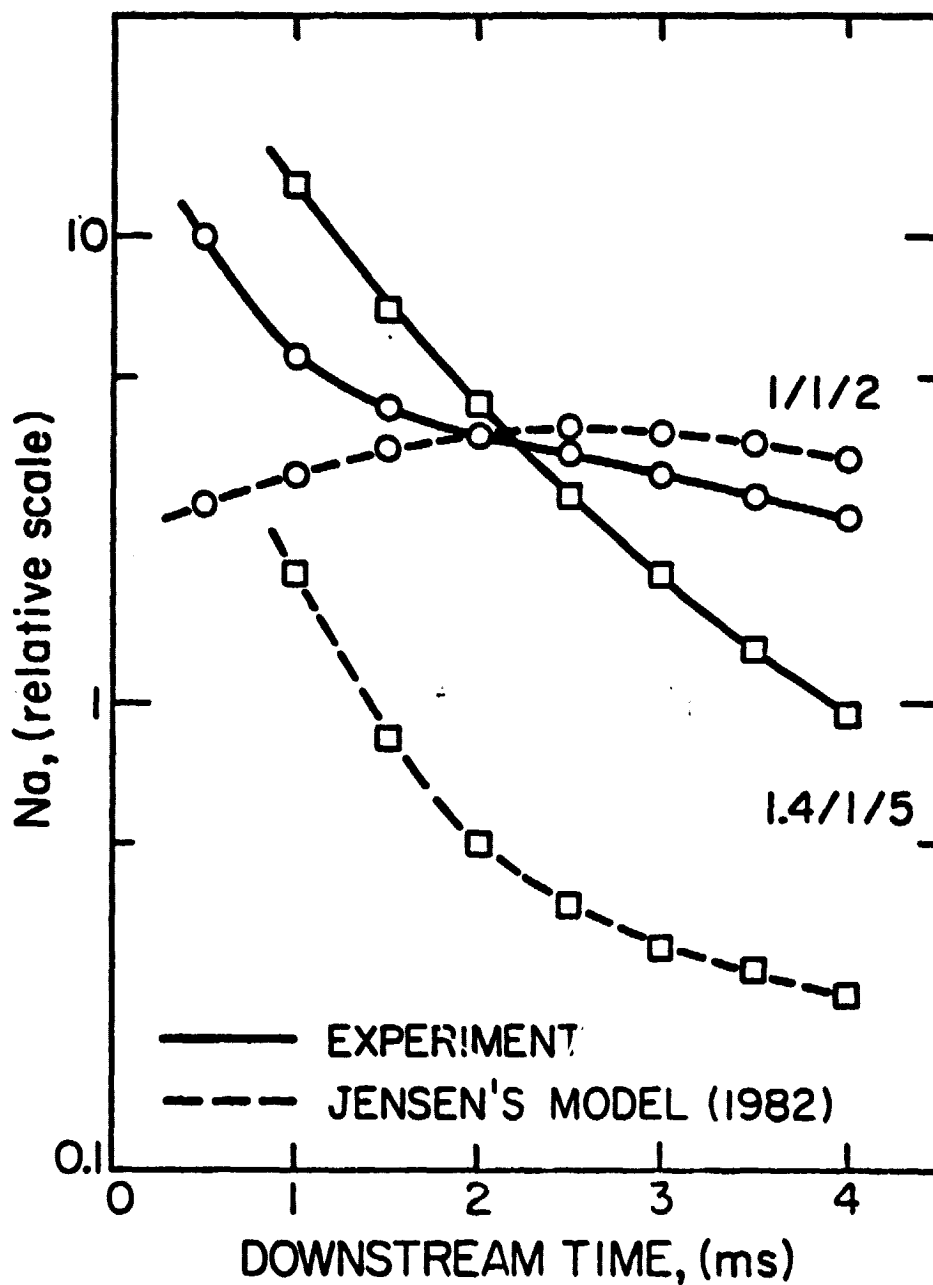
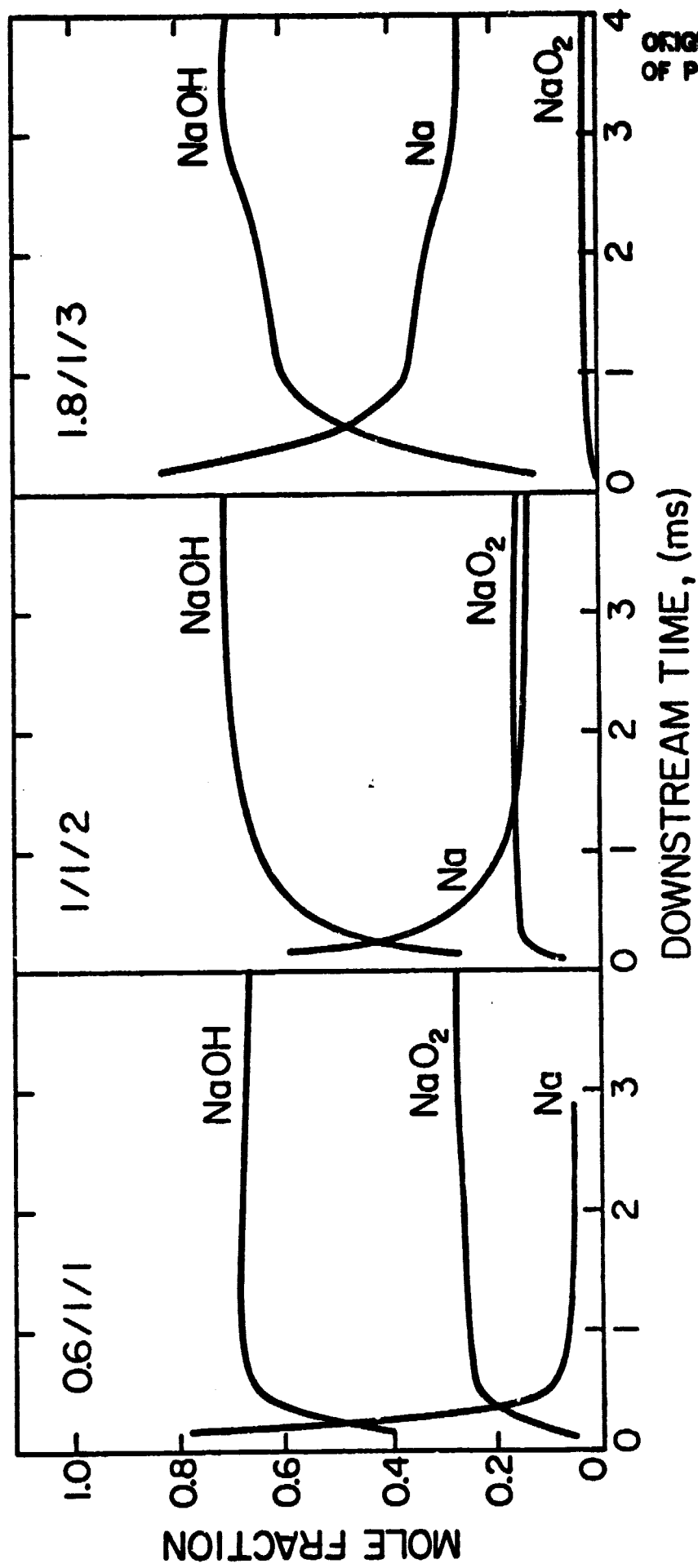


Figure 9. Predicted sodium concentrations based on Jensen's NaOH model compared to experimental values.

in Figure 10, although NaOH does consistently appear to be the dominant molecular form as suggested by Jensen, the role of NaO₂ cannot be ignored particularly at temperatures of <2000K. Consequently, in spite of its weak molecular structure, its rapid rate of production can maintain a significant steady state population.

Further refinements of our model, specifically to examine the effects of significantly increasing the rate constant of k_{13} as implied by Jensen and Jones⁸ now are in progress.

ORIGINAL PAGE IS
OF POOR QUALITY



ORIGINAL PAGE IS
OF POOR QUALITY

Figure 10. Predicted distributions among the sodium species in various flames for our optimum fit to the complete kinetic scheme.

ACKNOWLEDGMENTS

The authors are most grateful to Jerry Schofield for his programming skills and help in reducing this data.

This research has been supported in part by the NASA Lewis Research Center under Grant No. NSG 3256 and by the Department of Energy under Contract No. DE-AM03-76 SF 00034; PA 372.

REFERENCES

1. H. Smith and T.M. Sugden, Proc. Roy. Soc. A219, 204 (1953).
2. E.M. Bulewicz, C.G. Jones, and T.M. Sugden, Proc. Roy. Soc. A235, 89 (1956).
3. W.E. Kaskan, Symp. (Int.) on Combustion 10, 41 (1965).
4. M.J. McEwan and L.F. Phillips, Trans. Faraday Soc. 62, 1717 (1966).
5. G.J. Dougherty, M.J. McEwan, and L.F. Phillips, Combust. Flame 21, 253 (1973).
6. R. Carabatta and W.E. Kaskan, J. Phys. Chem. 72, 2483 (1968).
7. D. Husain and J.M. Plane, J. Chem. Soc. Faraday Trans. II, 78, 163 (1982).
8. D.E. Jensen and G.A. Jones, J. Chem. Soc. Faraday Trans. I, 78 (1982) (in press).
9. D.E. Jensen, J. Chem. Soc. Faraday Trans. I, 78 (1982) (in press).
10. C.H. Muller III, K. Schofield, M. Steinberg, and H.P. Broida, Symp. (Int.) on Combustion, 17, 867 (1979).
11. C.H. Muller, K. Schofield and M. Steinberg, J. Chem. Phys. 72, 6620 (1980).
12. P.J. Padley and T.M. Sugden, Proc. Roy Soc. A248, 248 (1958).
13. M.B. Denton and D.B. Swartz, Rev. Sci Instrum. 45, 81 (1974).
14. K. Schofield and M. Steinberg, Opt. Eng. 20, 501 (1981).
15. C.H. Muller III, K. Schofield, and M. Steinberg, in "Laser Probes for Combustion Chemistry," Am. Chem. Soc. Symp. Series 134, 103 (1980).
16. D.L. Hildenbrand and F. Murad, J. Chem. Phys. 53, 3403 (1970).
17. L. Andrews, J. Phys. Chem. 73, 3922 (1969).
18. R.R. Smardzewski and L. Andrews, J. Chem. Phys. 57, 1327 (1972).